Retarding the breaching process of dikes

Lemmens, D.; Bisschop, Rik; Visser, Paul; van Rhee, Cees

DOI
10.1680/jmaen.2015.20

Publication date
2016

Document Version
Final published version

Published in
Proceedings of the Institution of Civil Engineers - Maritime Engineering

Maritime Engineering

Retarding the breaching process of dikes
Lemmens, Bisschop, Visser and Van Rhee

ice | proceedings

Proceedings of the Institution of Civil Engineers

http://dx.doi.org/10.1680/jmaen.2015.20
Paper 201520
Received 17/07/2015 Accepted 07/04/2016
Keywords: failure/granular materials/sea defences

ice Institution of Civil Engineers
publishing

Retarding the breaching process of dikes

Dennis D. M. M. Lemmens
Production Engineer, Engineering and Estimating Department, Van Oord Marine Ingenuity, Rotterdam, the Netherlands (corresponding author: dennis@dlemmens.nl)

Rik Bisschop
Section Dredging Engineering, Faculty of Mechanical, Maritime and Materials Engineering and Faculty of Civil Engineering and Geosciences, Delft University of Technology, Delft, the Netherlands; Department of Hydraulic Engineering, Faculty of Civil Engineering and Geosciences, Delft University of Technology, Delft, the Netherlands; ARCADIS, Rotterdam, the Netherlands

Paul J. Visser
Department of Hydraulic Engineering, Faculty of Civil Engineering and Geosciences, Delft University of Technology, Delft, the Netherlands

Cees Van Rhee
Section Dredging Engineering, Faculty of Mechanical, Maritime and Materials Engineering and Faculty of Civil Engineering and Geosciences, Delft University of Technology, Delft, the Netherlands; Department of Hydraulic Engineering, Faculty of Civil Engineering and Geosciences, Delft University of Technology, Delft, the Netherlands

Dikes constructed from sand generally have a sand core and clay layers on the slopes and the crest to protect the core against erosion. In extreme hydraulic conditions, several failure mechanisms can lead to destruction of the clay layers, exposing the sand core to water. When water overtops the dike and the protective cover of the land-side slope or the crest fails, water flows over the core and erodes the sand. The dike starts to breach, and eventually the land behind the dike is flooded. The rate at which the dimensions of the breach grow influences the rate of inundation of the polder. Reduction of the inundation rate may be achieved by retarding the breaching process. This may reduce the number of casualties, resulting in increasing safety for the inhabitants. In order to achieve, for instance, a safety level ten times higher, mortality has to decrease by a factor of 10. The breaching process can be retarded by reducing the erosion velocity of the sand core. Experiments were executed to investigate the effect on the erosion velocity of adding bentonite to sand. The results of these experiments showed a significant reduction of the permeability and erosion velocity of the sand–bentonite mixtures compared with those of pure sand. The effect of adding bentonite on the breaching process was investigated by applying the Bres model (breach erosion in sand dikes model) to a sand dike tested in a large-scale field experiment (Zwin'94). It was found that adding a small percentage of bentonite reduces the rate of breach growth and the inundation rate in the polder. For the Zwin'94 dike it was determined that 5·4% of bentonite is sufficient to reduce the inundation rate below a threshold value of 0·5 m/h, leading to a significant increase in safety.

Notation

c_b	near-bed concentration (dimensionless) (volume concentration)
D_*	particle parameter (dimensionless)
D_{50}	particle diameter (m)
f	bulk friction (dimensionless)
f_b	bed friction (dimensionless)
$f_{evacuation}$	fraction of inhabitants evacuated (dimensionless)
f_w	wall friction (dimensionless) (curve fitting function)
$\boldsymbol{g}$	acceleration due to gravity (m/s^2)
h	water depth (m)
k	permeability (m/s)
k_{sand}	permeability of sand (m/s) (calculated in the Bres model)
k_{sb}	permeability of sand–bentonite mixture (m/s)
M_A	mortality, casualties as a fraction of all inhabitants of the flood zone
M_L	mortality, casualties as a fraction of inhabitants left in the flood zone
n	porosity (dimensionless)
n_i	maximum porosity of the sand (dimensionless)
P_F	probability of inundation of the relevant area
R	hydraulic radius of the total flow area (m)
S	energy slope (m/m)
$\boldsymbol{U}$	depth-averaged flow velocity (m/s)
$\boldsymbol{v}_e$	erosion velocity (m/s)
$\boldsymbol{v}_i$	inundation velocity (m/h)
$\boldsymbol{v}_{i\text{-}sand}$	inundation velocity for the sand dike (m/h)
w	width of the flow (m)
$\boldsymbol{w}_s$	hindered settling velocity of sand (m/s)

β	angle of bed slope (degrees)
Δ	relative density (dimensionless)
θ	Shields parameter (dimensionless)
θ_c	critical Shields parameter (dimensionless) (Van Rijn, 1984)
ν	kinematic viscosity of water (m^2/s)
ξ_b	weight fraction of added bentonite (dimensionless)
ρ	water density (kg/m^3)
$\boldsymbol{\tau}$	shear stress (Pa)
$\boldsymbol{\tau}_a$	total shear stress (Pa)
$\boldsymbol{\tau}_b$	bed shear stress (Pa)
ϕ	angle of internal friction (degrees)

1. Introduction

Dikes have failed in the past all over the world, and will continue to do so in the future. Failures can happen during extremely high river or sea levels. In most cases, dikes are protected by protective covers or revetments, but if these fail, a dike may start to breach. This is especially the case for sand dikes, in which a major breach can form within a few hours after the failure of the protective cover (Visser, 1998). In such an event, water will enter the polder behind the dike and the area will be inundated. This flooding causes casualties and economic damage. Most casualties of such a flood are caused by relatively large flow velocities and rapidly rising water levels in the polder. These inundation parameters depend on the development of the discharge through the breach, and thus on the speed of the breach growth process and the area of the polder (Rijkswaterstaat, 2006). Usually, dikes are constructed such that they are sufficiently high and strong enough to minimise the chance of an inundation. This can be costly and space-consuming, and, in the case of breaching of the dike, the dike failure is generally still brittle so that there is little time to battle the failure to reduce the consequences. Instead of increasing the crest height and the related dimensions of a dike, there are other ways to strengthen a dike and to reduce the number of casualties if it fails.

One of these ways is to take measures that will retard the breaching process so that the dike will fail in a more gradual way. The breaching process can be slowed down by reducing the erosion velocity of the sand in the sand core. Due to this ductile failure, the breaching process will be more gradual and the consequences will be reduced.

2. Breaching process and safety level

The breaching process often starts with erosion of the inner (land-side) slope. This inner slope has a protective cover of clay and grass to prevent this erosion. The dike will not erode as long as the cover stays intact. It is, however, possible that the cover is damaged (e.g. by wave overtopping, piping, macro- or micro-instability) and the sand core of the dike is then exposed to water and waves. When that happens, the dike core starts to erode and a breach will develop.

In breach models, it is often assumed that the breaching process starts (at time $t = t_0$) with an initial breach in the crest of the dike (made on purpose as an initial breach or pilot channel in experiments or representing damage to the protective cover during a real breaching event). Water will flow through this initial breach (in critical flow conditions), initiating the breaching process of the core. Five stages (Figure 1) can be distinguished in this process (Visser, 1998).

- Stage I (from t_0 until t_1). The (supercritical) flow velocity along the inner slope increases. As a result, erosion increases along the slope, increasing the angle of the inner slope from an initial value of β_0 to a critical value of β_1 at $t = t_1$ (the critical angle may be the internal friction angle, although Visser (1998) notes that steeper slopes have been observed).
- Stage II (from t_1 until t_2). The erosion of the inner slope continues at the critical angle β_1 (retrograde erosion), reducing the width of the dike crest in the breach. This continues until the crest width has become zero at t_2.
- Stage III (from t_2 until t_3). During this stage, the remainder of the dike core in the breach is eroded down to the base of the dike (or the berm on the outer slope (Visser, 1998)). Consequently, the width of the breach also increases, as the side slopes of the breach maintain a critical angle γ_1. This stage ends at t_3 when the bottom of the breach has reached the level of the base of the dike.
- Stage IV (from t_3 until t_4). The critical flow through the breach continues to erode the breach, mainly horizontally but also vertically. The vertical erosion depends on the erodibility of the base of the dike and is usually small compared with the lateral erosion. As in stage III, the side slopes of the breach remain at the critical angle γ_1. This stage ends at t_4 when the flow through the breach becomes subcritical due to the rising water level in the polder.
- Stage V (from t_4 until t_5). In this subcritical flow stage, the breach continues to grow (mainly) laterally, with breach side slopes remaining at the critical angle γ_1. In this stage, the water level in the polder continues to rise and the difference between the outside water level and the inside water level decreases. This reduces the flow velocity through the breach, and eventually the velocity becomes too low to pick up sand particles, stopping the erosion process and thus the breaching process at t_5. The flow through the breach stops at t_6 when the inside water level equals the outside water level.

The breaching process described above was modelled on the Bres model (breach erosion in sand dikes model; 'bres' is also the Dutch word for breach (Visser, 1998)). Besides the Bres model, there are several breaching models available for sand, clay and composite dikes and dams (Morris *et al.*, 2009). The Bres model was chosen due to its relevance to sand dikes,

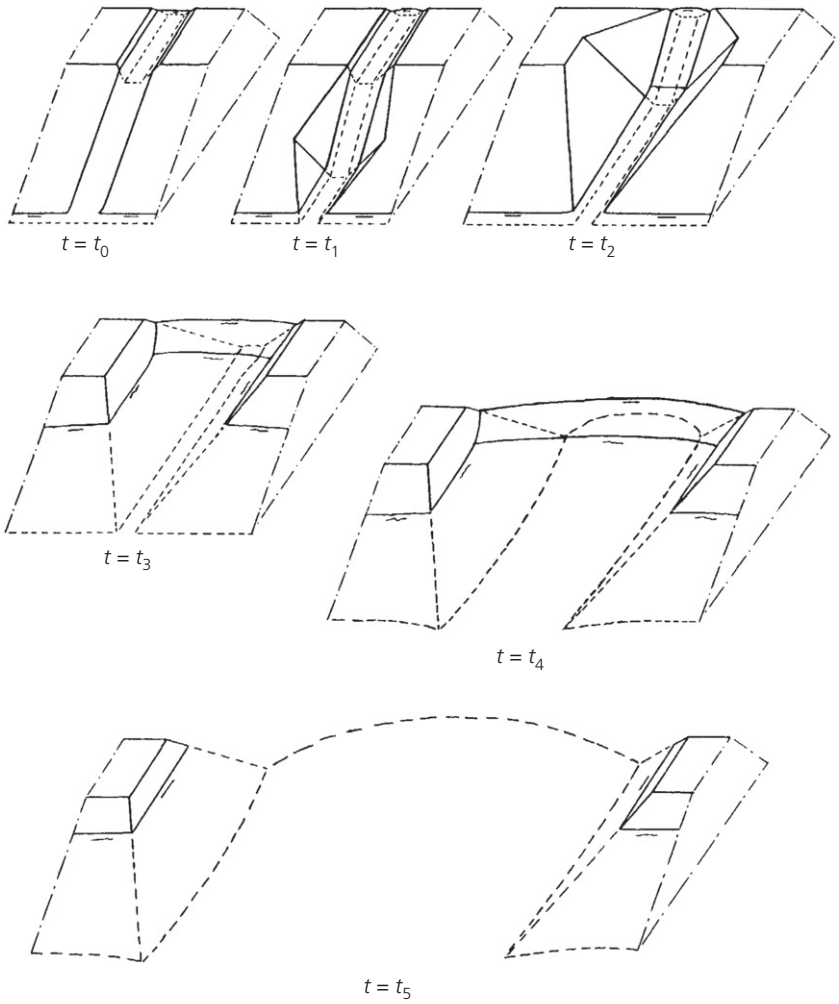

Figure 1. Schematic overview of the breaching process of a sand dike (Visser, 1998)

the SWOT (strengths, weaknesses, opportunities and threats) analysis of Peeters *et al*. (2011), its good performance in engineering practice and its availability to the authors. For a more detailed explanation of the set-up and limits of the Bres model, reference is made to Visser (1998).

In the Netherlands, inundation probability (P_I) is determined as the probability of exceedance of a maximum water level in front of the dike (P_E) multiplied by the probability of failure of the dike (P_F): $P_I = P_E P_F$. A drawback of this definition is that it does not take mitigating measures into account. Therefore, the definition was changed to the probability of the loss of life of a person as a result of a dike failure. This new definition makes it possible to define a more accurate and local level of safety. It includes all relevant failure mechanisms, evacuation, mitigating measures and so on. It is then possible to define the desired decrease of mortality to increase the level of safety. A formula used to derive the safety level is the localised individual risk (LIR) of loss of live due to a flood (Deltares, 2011)

$$\text{LIR} = P_F(1 - f_{\text{evacuation}})M_A = P_F M_L \quad (1)$$

in which $f_{\text{evacuation}}$ is the fraction of inhabitants evacuated, M_A is mortality in terms of casualties as a fraction of all inhabitants of the flood zone, M_L is the mortality in terms of casualties as a fraction of inhabitants left in the flood zone and P_F is the probability of inundation of the relevant area.

To increase safety by a factor of 10, the LIR has to be reduced by a factor of 10. This can be achieved by decreasing mortality by a factor of 10 as well. Research into loss of life due to flood events (Jonkman, 2007) shows that mortality increases with

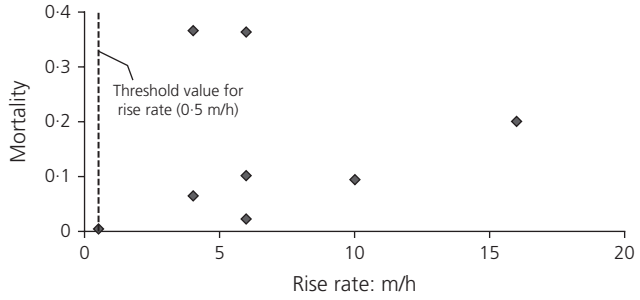

Figure 2. Mortality due to inundation velocity (rise rate) (Jonkman, 2007)

inundation speed. This rise rate has an estimated threshold value of 0·5 m/h for mortality, as shown in Figure 2. Mortality, and thus the LIR, can be reduced by slowing down the breaching process.

The breaching process of a sand dike can be slowed down by reducing the erosion velocity of sand. There are several methods available to reduce the erodibility of sand – such as grouting or biological cementation of the sand in a dike – which have been compared by means of a literature study (Lemmens, 2014). The study concluded that adding bentonite is the best method, based on adequate substantiated scientific studies. Bentonite reduces the permeability and therefore the erodibility of sand (Gailani *et al.*, 2001). During erosion, water needs to flow into the pores to pick up grains. By reducing this inflow, the erosion velocity can be reduced.

3. Experiments

Experiments were conducted by Lemmens (2014) to test whether bentonite can reduce the erosion velocity of sand and retard the breaching process. The experiments were executed for clean sand and sand mixed with bentonite. The main goal of the experiments was to determine whether there is a difference in erosion velocity between sand and different sand–bentonite mixtures. The secondary goal of the experiments was to determine whether the additives influence relevant soil parameters such as shear strength and permeability.

3.1 Materials

The sand used for the tests and for mixing is a pure quartz sand ($D_{50} = 208$ μm). The coefficient of uniformity (C_u) and coefficient of curvature (C_c) are 1·7 and 1·0, respectively, hence the sand can be classified as poorly graded according to Holtz and Kovacs (1981).

The sand–bentonite mixtures were prepared by mixing sand and bentonite using a concrete mixer. The materials were dry mixed in batches of ∼25 kg (weight of one bag of sand and additive).

	ϕ: degrees	c: kPa
Sand	34·6	0·70
Sand–bentonite (1·2%)	34·3	0·80
Sand–bentonite (2·4%)	36·7	0·03

Table 1. Friction angle (ϕ) and (apparent) cohesion (c) of the mixtures

	k: m/s	k/k_{sand}: dimensionless
Sand	$1{\cdot}91 \times 10^{-4}$	1·00
Sand–bentonite (1·2%)	$7{\cdot}07 \times 10^{-5}$	0·37
Sand–bentonite (2·4%)	$3{\cdot}08 \times 10^{-5}$	0·16

Table 2. Permeability coefficients (k) and reduction ratio (k/k_{sand}) of permeability of the mixtures relative to sand

For mixing, Cebogel Sealfix bentonite (Cebo Holland BV, 2014) was used. This bentonite is already being used in practice to create sand–bentonite seals. It is a powder of activated sodium bentonite, which has a high swell capacity. Two mixtures with different weight percentages were tested during these experiments, 1·2% and 2·4% mass of bentonite of the total dry mass.

3.2 Geotechnical tests

The shear strength of the sand and the two mixtures was determined by direct drained shear tests (Table 1).

It can be concluded from Table 1 that the (apparent) cohesion of both mixtures was very small and that only the mixture with 2·4% bentonite had a small increase in the friction angle. Therefore, it can be concluded from this test that both mixtures behave like sand and thus can be modelled like sand.

Falling head tests were executed to determine the permeability of the sand and the two mixtures. The results are given in Table 2.

Table 2 shows that adding bentonite to sand decreases the permeability significantly. For 1·2% of bentonite, the permeability reduced to about 1/3 of that of sand without bentonite; 2·4% of bentonite gave a reduction with a ratio of about 1/6. Figure 3 shows an empirical relation to derive the relative permeability (k/k_{sand}) of a sand–bentonite mixture. The reduced permeability of the sand–bentonite mixtures is expected to decrease erosion velocities, which were tested in the erosion experiments.

3.3 Erosion experiment

The erosion tests were performed in a flume at the Laboratory of Fluid Mechanics of Delft University of Technology.

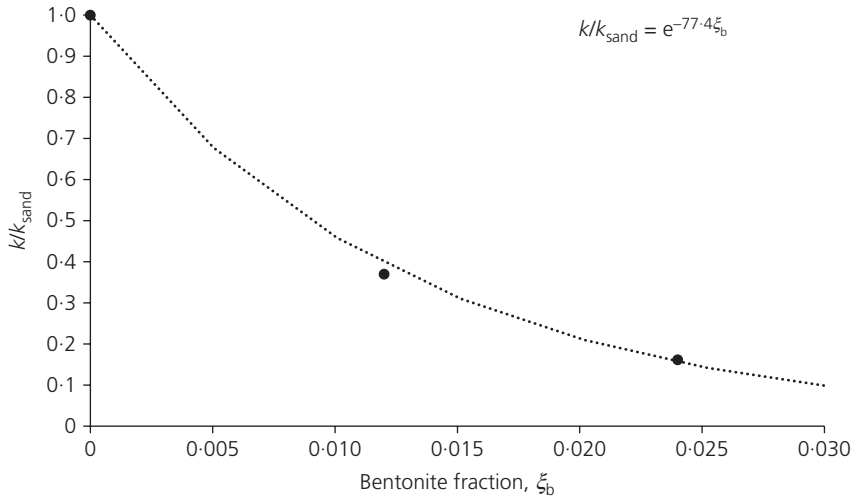

Figure 3. Reduction of permeability as a function of weight fraction of added bentonite

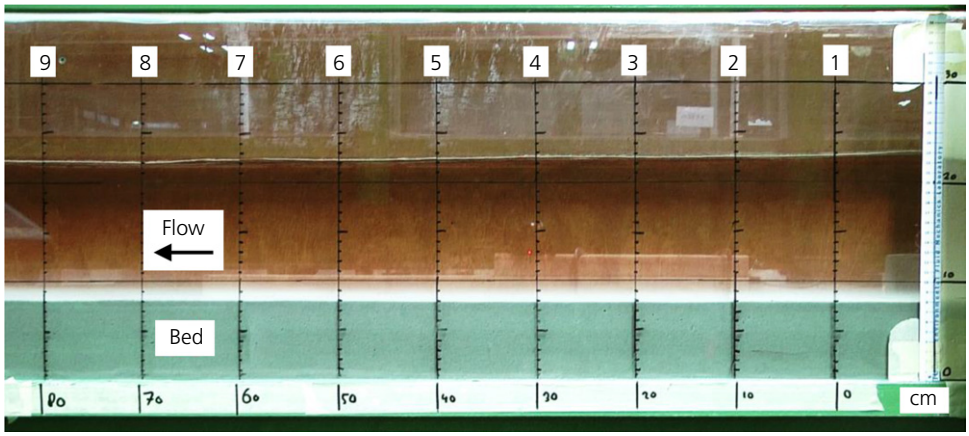

Figure 4. Measurement area and measurement locations (1–9)

The flume has a length of 4·4 m, a width of 0·105 m and a height of 0·4 m. Flow into the flume is driven by gravity, from a reservoir in the laboratory, through a pipe into the flume. A magnetic flow meter was used to measure the discharge through the pipe. In each test, the rate of flow over the bed was constant. The side walls of the flume were made from glass panels. The water levels and bed levels were observed through one of these panels (Figure 4) with a video camera, from the start until the end of each test. Figure 4 also shows the grid drawn on the panel and the measurement area with nine measurement locations. The video recordings allowed determination of the erosion velocities of the bed and, with the known discharge and the flume width, determination of the depth-averaged flow velocities. The erosion velocity, which is defined as the vertical velocity of the bed level, was determined by measuring the bed level at set intervals (by means of the video recording) and then dividing the difference in bed levels by the set time interval.

The bed of sand or mixture was prepared at a dry bulk density of ~1600 kg/m^3 (resulting in a porosity of 0·40). The bed, with a length of 3·4 m, was compacted by hand and by means of a wooden tool and hammer. Due to inconsistency in the compaction method, a small spread in the dry bulk densities (between 1482 and 1667 kg/m^3) and therefore the porosities (between 0·37 and 0·40) occurred over the tests. After preparation of the bed, water was kept on top of the bed for an extended period of time to allow saturation of the bed. For the

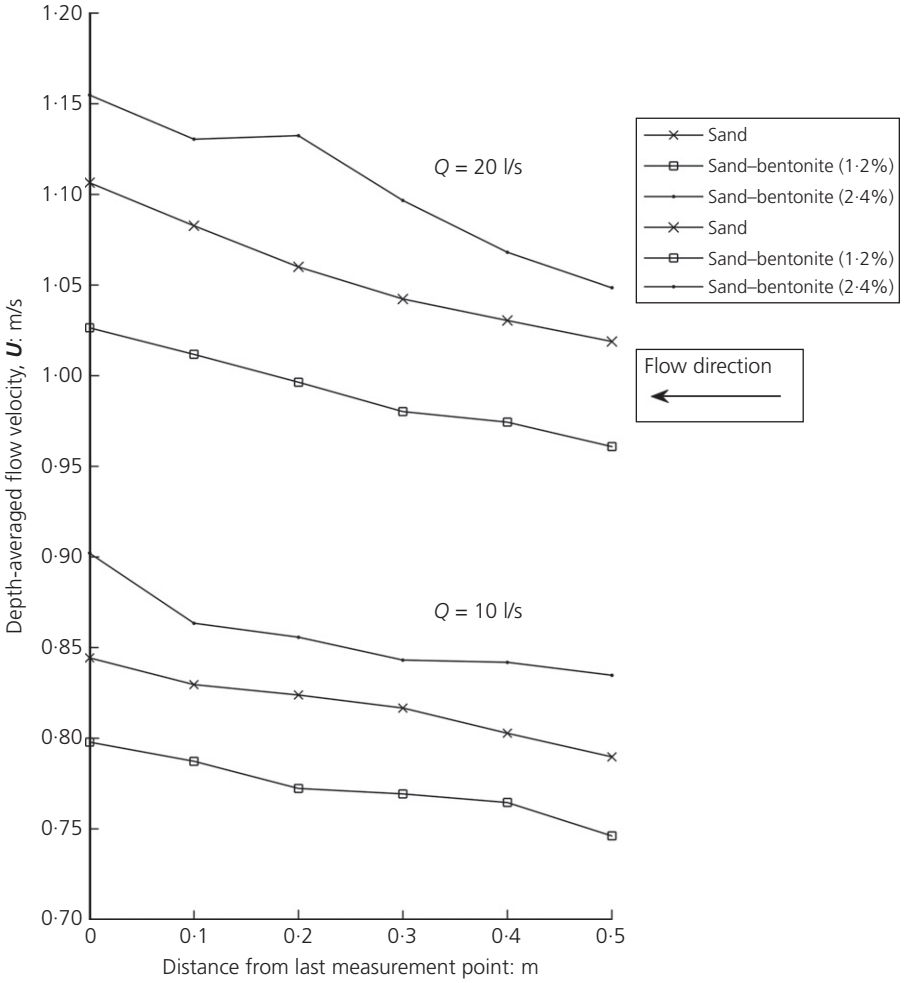

Figure 5. Depth-averaged flow velocities per test (measurement locations 4 = 0·5 m to 9 = 0 m)

sand–bentonite mixtures, this was particularly important, since the bentonite needs time to swell to its full capacity. The tests were executed at two different flow rates ($Q = 10$ l/s and $Q = 20$ l/s) for each mixture. Due to differences between the tests (e.g. bed density), the depth-averaged flow velocities varied over the tests, as shown in Figure 5. Turbulence in the inflow section yielded inaccurate measurements in measurement locations 1, 2 and 3 and these data were not included in Figure 5.

In all the tests, the depth-averaged flow velocities increased in the flume, thus the flow accelerated. This acceleration was induced by the adaptation distance of the flow being longer than the length of the flume, resulting in the flow still reaching equilibrium in the flume. The depth-averaged flow velocities increased irregularly (Figure 5), most likely caused by turbulence in the flow. This turbulence in the flow was partly caused by the water depth reduction due to the presence of the bed at the beginning of the flume. This was particularly noticeable during the higher velocity tests ($\boldsymbol{U} > 1$ m/s). A part of the spread in the results can be explained by this turbulence.

4. Results

With the data of water level and bed level measurements, the depth-averaged flow velocities and erosion velocities were determined. These were used to create linear regression lines, which were used to calculate the erosion velocity as a function of depth-averaged flow velocity for each mixture. Figure 6 shows these linear regression lines for all tests, including the erosion velocity at the depth-averaged flow velocity $\boldsymbol{U}$ during each test.

Figure 6 shows the effect of adding 1·2% bentonite to the sand on the erosion velocity. Adding a small amount of

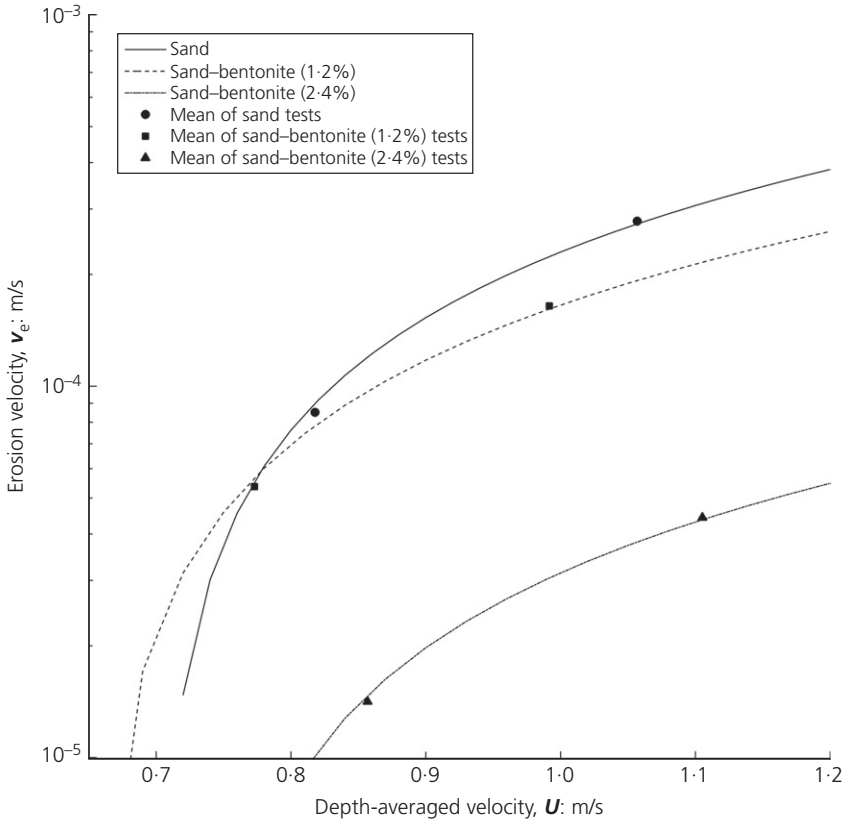

Figure 6. Linear regression lines and mean results of erosion experiment

bentonite (1·2%) decreases the erosion velocity slightly for depth-averaged flow velocities U larger than about 0·8 m/s (for $U = 1{\cdot}2$ m/s the erosion velocity reduces with 30%), but increases erosion velocities for $U < 0{\cdot}8$ m/s. Adding 2·4% of bentonite, however, reduces the erosion velocity significantly – that is, with a ratio of about 0·12 (Table 3) for all depth-averaged flow velocities. It should be noted that (*a*) in the present experiment only two mixture ratios were tested, and other mixture ratios might give better results and (*b*) the present tests were executed at relatively low depth-averaged flow velocities, so the mixtures need to be tested at higher flow velocities to determine the effect at these flow velocities.

For all tests, linear regression lines for the erosion velocity as a function of U^2 were also determined. The U^2-axis crossings at $v_e = 0$ m/s were also calculated, as shown in Figure 7. These U^2 values are proportional to the critical shear stress and are an indication of the critical shear velocity.

Since both the critical U values and the critical U^2 values were similar for the different mixtures and sand, the erosion processes were considered to be similar. If this was not the case, large deviations in the critical velocities should be noticeable – for example, those caused by a significant cohesion of a mixture.

	Sand–bentonite (1·2%)	Sand–bentonite (2·4%)
f_r ($U \approx 0{\cdot}8$ m/s)	0·88	0·11
f_r ($U \approx 1{\cdot}1$ m/s)	0·70	0·14

Table 3. Reduction ratio (f_r) of erosion velocity of mixtures relative to sand

5. Analysis

The bed shear stress was derived from measurements of the total pressure and energy loss during the erosion tests. In order to derive the effect of bed shear stress, the measured pressure gradient was corrected for the acceleration of the flow and the influence of the friction along the wall of the flume.

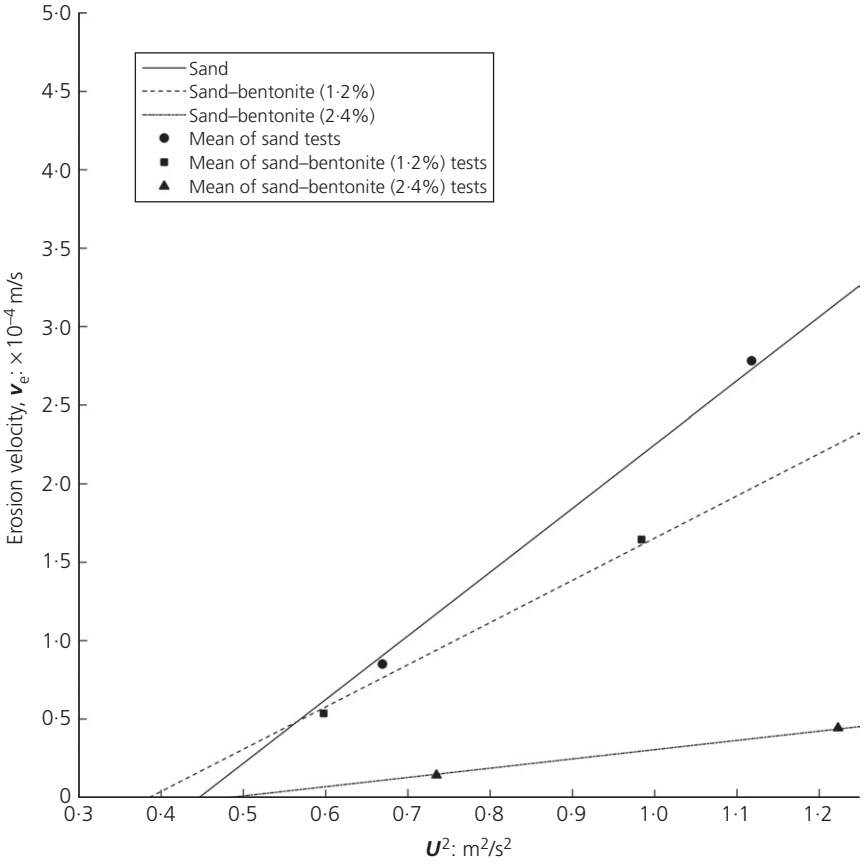

Figure 7. Crossing of U^2-axis at $v_e = 0$ m/s of the linear regression lines (with mean results of experiments)

For each test, the water depth at six different locations was measured (measurement locations 4–9). These water depths were used to calculate the depth-averaged flow velocities during each test. For each measurement location, the time-averaged and depth-averaged flow velocity and average water depth were known, and were used to calculate the hydraulic radius (R), energy height (H) and pressure (p).

The pressure gradient ($\mathrm{d}p/\mathrm{d}x$) is corrected for the acceleration of the flow using the method described by Van Rhee and Talmon (2010)

$$2.\quad \frac{\mathrm{d}p}{\mathrm{d}x} = \frac{\mathrm{d}h}{\mathrm{d}x}\rho g = -\tau_a \frac{1}{R} - \frac{\mathrm{d}}{\mathrm{d}x}(\rho U^2) = -\tau_a \frac{1}{R} - U^2 \frac{\mathrm{d}\rho}{\mathrm{d}x} - \rho \frac{\mathrm{d}U^2}{\mathrm{d}x}$$

in which h is the water depth (m), R is the hydraulic radius of the total flow area (m), U is the depth-averaged flow velocity (m/s), ρ is the water density (kg/m^3) and τ_a is the total shear stress (Pa).

Equation (2) also comprises a term for the density gradient ($\mathrm{d}\rho/\mathrm{d}x$). This gradient was assumed to be zero for the executed tests because the effect of erosion on the increase of the density of the eroding flow was negligible. By rewriting Equation (2) and neglecting the term ($\mathrm{d}\rho/\mathrm{d}x$), an expression for the total shear stress (τ_a (Pa)) is found

$$3.\quad \tau_a = -R\left(\frac{\mathrm{d}\tilde{p}}{\mathrm{d}x}\right)$$

with

$$4.\quad \frac{\mathrm{d}\tilde{p}}{\mathrm{d}x} = \frac{\mathrm{d}h}{\mathrm{d}x}\rho g - \rho \frac{\mathrm{d}U^2}{\mathrm{d}x}$$

The total shear stress was determined based on the pressure gradient ($\mathrm{d}p/\mathrm{d}x$) corrected for the acceleration of the flow, which is the corrected pressure gradient ($\mathrm{d}h/\mathrm{d}x - \rho \mathrm{d}U^2/\mathrm{d}x$).

The method used for calculating the bed shear stresses of the tests was the Vanoni and Brooks formula (Cheng and Chua, 2005). Equation (5) was selected since it applies the necessary corrections for wall friction

$$5. \quad \tau_b = \frac{w}{w+2h}\frac{f_b}{f}\frac{1}{\rho g h S}$$

$$6. \quad f = \frac{8gRS}{U^2}$$

$$7. \quad f_b = f + \frac{2h(f-f_w)}{w}$$

$$8. \quad f_w = \left(20\left(\frac{4UR/v}{f}\right)^{0\cdot1} - 39\right)^{-1}$$

in which f is the bulk friction (dimensionless), f_b is the bed friction (dimensionless), f_w is the wall friction (curve fitting function) (dimensionless), g is acceleration due to gravity (m/s^2) (= 9·81 m/s^2), R is the hydraulic radius of the total flow area (m), S is the energy slope (m/m), w is the width of the flow (m), v is the kinematic viscosity of water (m^2/s), ρ is the water density (kg/m^3) and τ_b is the bed shear stress (Pa).

The bed shear stresses were converted to a Shields parameter (θ) (Van Rijn, 1984)

$$9. \quad \theta = \frac{\tau}{\rho g \Delta D_{50}}$$

in which D_{50} is the particle diameter (m), Δ is the relative density (dimensionless) (= 1·65) and τ is the shear stress (Pa).

Due to the decreasing permeability, the erosion velocity decreases. The flow conditions during the erosion tests were in the sheet flow regime ($\theta > 0{\cdot}3$–1). In this regime, the erosion process is dominated by the shearing of layers of sand. Sand layers will dilate before shearing, and water has to flow between the grains to fill the voids. This effect is evident from the results of the tests. From the permeability tests it can be concluded that the permeability of sand decreases with increasing bentonite content, while the erosion tests showed that the erosion rate decreased with increasing bentonite content. The lower permeability of sand with a high bentonite content hinders the inflow of water into the sand bed, hence reducing the erosion rate. The resulting higher pressure gradient pushes grains into the bed, making it more difficult to erode the sand.

5.1 Erosion formula

The test results were compared with the erosion formula of Van Rhee (2010) (Figure 8). The Van Rijn–Van Rhee formula (Van Rhee, 2010) was used since it has corrections for bed slope and near-bed concentration, porosity and permeability, of which the latter is necessary to model the effect of sand–bentonite mixtures. Also, this formula is valid in the dilatancy-restricted erosion regime, which is the regime in which these experiments were executed. When implemented in the Bres model, the model produces results that are in good agreement with the experimental data (Bisschop *et al.*, 2010). Thus, for the sand used in the experiments, with or without bentonite, the erosion velocity can be calculated using the Van Rijn–Van Rhee erosion formula, given by Van Rhee (2010)

$$10. \quad v_e = \frac{1}{1-n-c_b}\left(\phi_p\sqrt{g\Delta D_{50}} - c_b w_s\right)$$

in which

$$11. \quad \phi_p = 0{\cdot}00033 D_*^{0\cdot3}\left(\frac{\theta-\theta_c^1}{\theta_c^1}\right)^{1\cdot5}$$

$$12. \quad \theta_c^1 = \theta_c\left(\frac{\sin(\phi-\beta)}{\sin(\phi)} + \delta_p\frac{v_e}{k}\right)$$

$$13. \quad \delta_p = \left(\frac{n_i-n}{1-n_i}\frac{1}{\Delta(1-n)}\right)$$

$$14. \quad D_* = D_{50}\left(\frac{\Delta g}{v^2}\right)^{1/3}$$

where c_b is the near-bed concentration (dimensionless) (volume concentration), D_* is the particle parameter (dimensionless), D_{50} is the particle diameter (m), k is the permeability (m/s) (= 1·91 × 10^{-4} m/s for the used sand), n is the porosity (dimensionless) (during sand tests ~0·38), n_i is the maximum porosity of the sand (dimensionless) (= 0·48), v_e is the erosion velocity (m/s), w_s is the hindered settling velocity of sand (m/s),

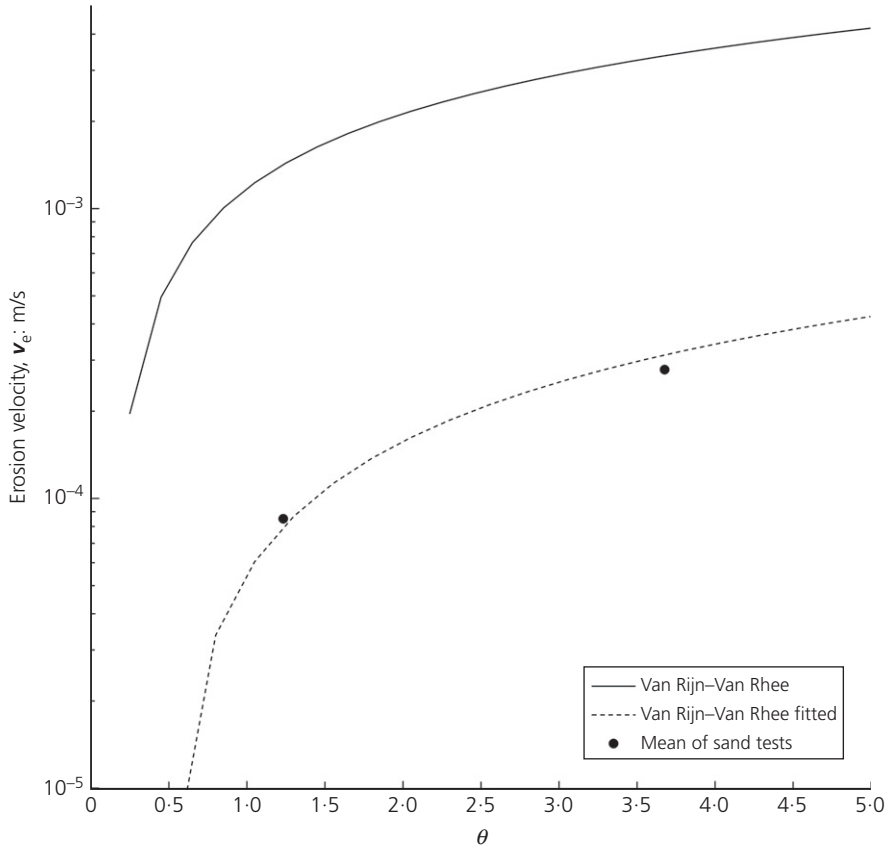

Figure 8. Comparison of test results with the Van Rijn–Van Rhee formula (Equation (10)) (for $c_b = 0$ and $k = k$) and fitted for the sand test (for $c_b \approx 0{\cdot}03$ and $k = k/20$)

ϕ is the angle of internal friction (degrees) (= 34°), β is the angle of bed slope (degrees) (= 0°), Δ is the relative density (dimensionless) (= 1·65) and v is the kinematic viscosity (m^2/s).

Using Equation (10), the erosion velocities were calculated for the same conditions as for those during the tests with pure sand. First this was calculated for clear water erosion, which means assuming a near-bed concentration of zero ($c_b = 0$). The Van Rijn–Van Rhee function does not match the measurements of the sand tests (Figure 9). A possible cause is the near-bed concentration, which was not zero during the tests. By adapting the near-bed concentration ($c_b \approx 0{\cdot}03$) and dividing the permeability by 20 ($k = k/20$), the calculated and experimental results match quite well, as Figure 9 shows (sand and fitted lines). The reduction in permeability is necessary to fit Equation (10) to the measurements and is not representative of the real value of the permeability. This reduction ratio is an empirical coefficient.

This fit was used to adapt Equation (10) to the sand–bentonite tests. This was achieved by dividing the permeability values of the sand–bentonite mixtures (1·2% or 2·4%), $7{\cdot}07 \times 10^{-5}$ or $3{\cdot}08 \times 10^{-5}$ m/s, respectively, by 20. By only adapting the permeability of the fitted formula, the calculated erosion velocities show a similar reduction as the test results (Figure 9). This makes the function suitable for modelling the erosion during the breaching process of a sand–bentonite dike.

6. Application

As described above, mixing sand with bentonite can significantly reduce the erosion velocity of sand. To investigate the effect of the reduced erosion velocity on the breaching process of sand dikes, the Bres model was applied to the sand dike of the Zwin'94 experiment (Visser, 1998). The data of the Zwin'94 experiment were used to calibrate the Bres model (Visser, 1998). Figure 10 shows a cross-section of this dike.

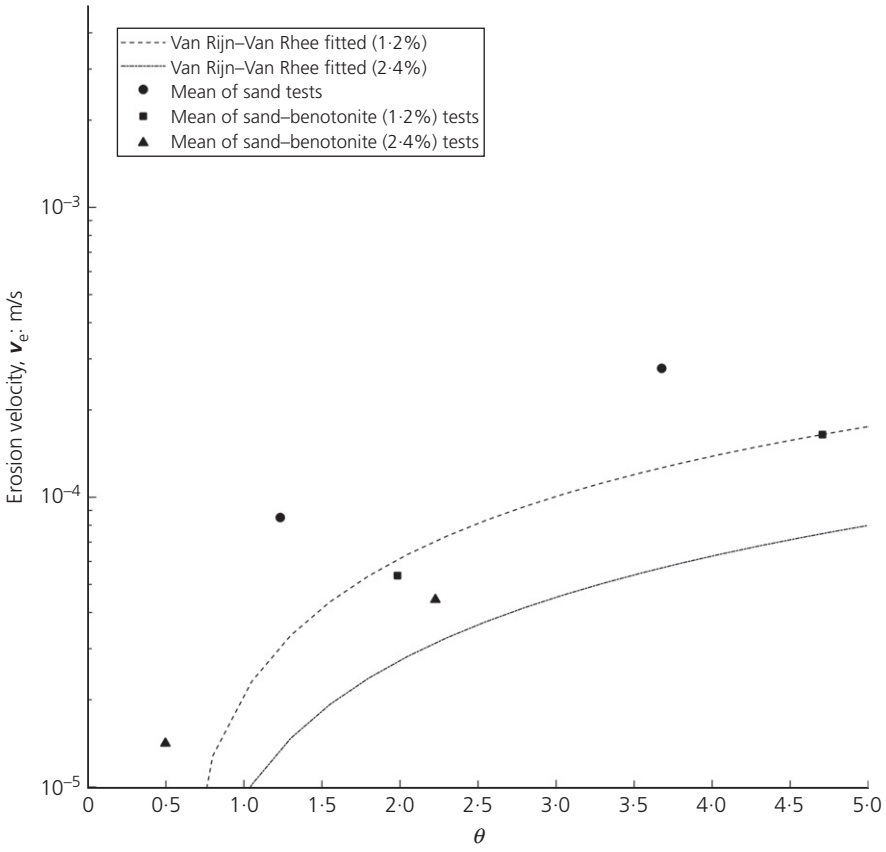

Figure 9. Fitting of the Van Rijn–Van Rhee formula (Equation (10)) (for $c_b \approx 0{\cdot}03$ and $k = k/20$) to the results of the sand–bentonite tests (1·2% and 2·4%), by using permeability to the values measured

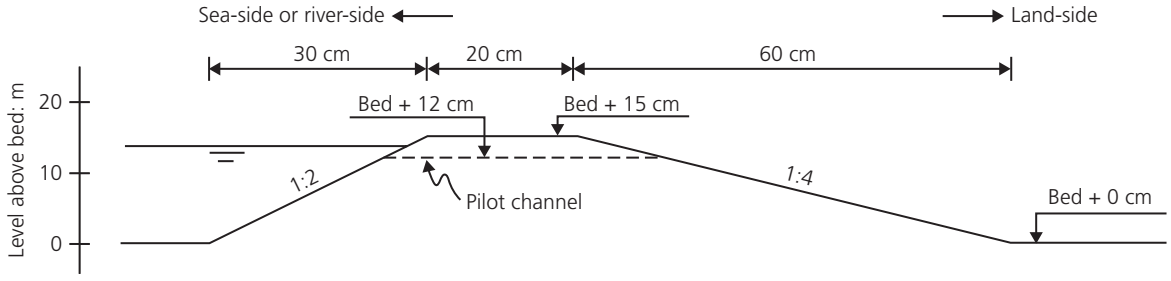

Figure 10. Cross-section of the Zwin'94 dike (Visser, 1998)

The effect of bentonite on the erosion velocity was modelled with the Van Rijn–Van Rhee erosion formula (Equation (10)) (Van Rhee, 2010), by adapting the permeability according to Figure 3. The reduction of permeability as a function of the weight percentage shown in Figure 3 can be approximated as

$$15. \quad k_{sb} = k_{sand} e^{-77{\cdot}4\xi_b}$$

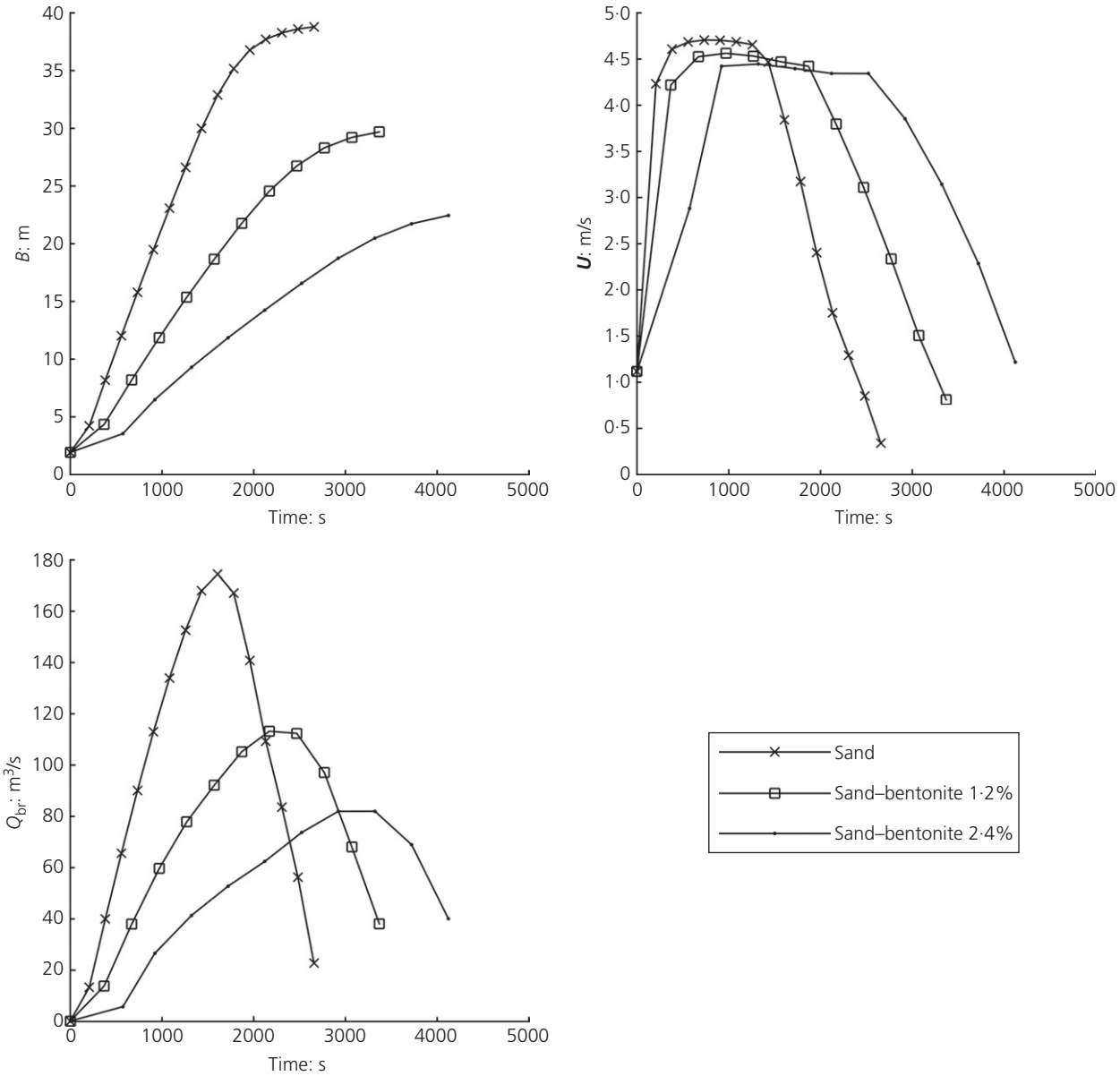

Figure 11. Comparison of results Bres model for the Zwin'94 dike for different added weight fractions of bentonite

in which k_{sand} is the permeability of the sand (m/s) (calculated in the Bres model), k_{sb} is the permeability of the sand–bentonite mixture (m/s) and ξ_b is the weight fraction of the added bentonite (dimensionless).

By implementing Equation (15) in the Bres model, the model simulates the breaching process for the different weight percentages of the added bentonite. This was done for the Zwin'94 dike for sand with 0, 1·2 and 2·4% of added bentonite. The effect of the different percentages of added bentonite on the breach width (B), breach discharge rate (Q_{br}), depth-averaged flow velocity ($\boldsymbol{U}$) and inundation velocity ($\boldsymbol{v}_i$) is shown in Figures 11 and 12. These figures show that the breach width, breach discharge rate and inundation velocity decrease with increasing bentonite percentage.

The model results show that a weight percentage of 2·4% of bentonite added to sand decreases the maximum values of the

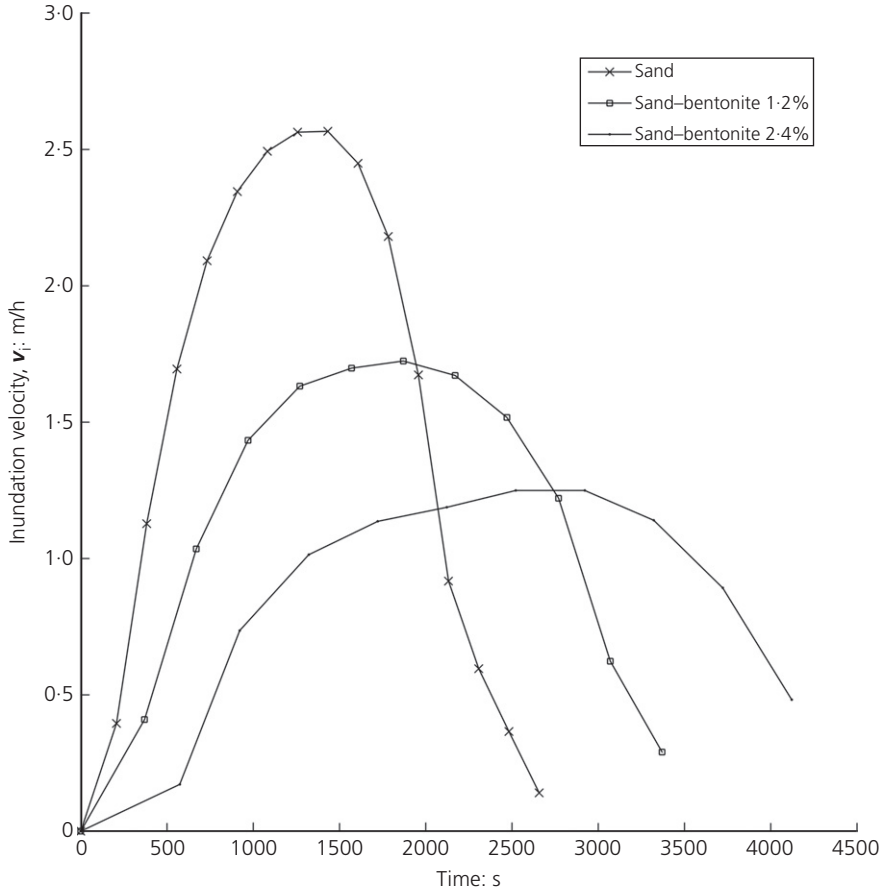

Figure 12. Comparison of inundation velocities in the Zwin'94 polder for different added weight fractions of bentonite

inundation parameters (breach width, breach discharge rate and inundation velocity) for the Zwin'94 dike by half. This is, however, not sufficient to lower the inundation velocity below the threshold value of 0·5 m/h. Based on the model and experimental results, it is possible to determine what weight percentage of bentonite would lower the inundation velocity below this threshold value for a normal dike.

6.1 Necessary mixture

On the basis of the results given by the Bres model for 1·2% and 2·4% of added bentonite, a relation between the weight fraction of added bentonite and a reduction ratio for the inundation velocity can be formulated

$$16. \quad \frac{v_i}{v_{i\text{-sand}}} = e^{-30{\cdot}2\xi_b}$$

in which v_i is the inundation velocity (m/h), $v_{i\text{-sand}}$ is the inundation velocity for the sand dike (m/h) and ξ_b is the weight fraction of added bentonite (dimensionless).

Equation (16) gives the reduction of the inundation velocity as a function of the weight fraction of added bentonite compared with the situation with no added bentonite. A reduction of the inundation velocity of more than 80% is necessary to reduce the inundation velocity for 0% bentonite to the threshold value of 0·5 m/h. Equation (16) predicts a bentonite percentage of 5·4% to obtain this reduction.

To verify that adding 5·4% of bentonite to sand would actually lead to an inundation velocity below the threshold value, the breaching process for this mixture was also simulated in the Bres model. However, in the Zwin'94 experiment, the measured outside water level (tide) dropped faster than the drop of the breach bottom in stage II predicted by the Bres model, thus stopping the breaching process in stage II. Stage III was never initiated since the outside water level was too low at that time step. For the Zwin'94 dike, this means it is possible to prevent a catastrophic breach of the dike by adding enough bentonite to the sand. This might be possible for other dikes as well, but will depend on case-specific circumstances. For each

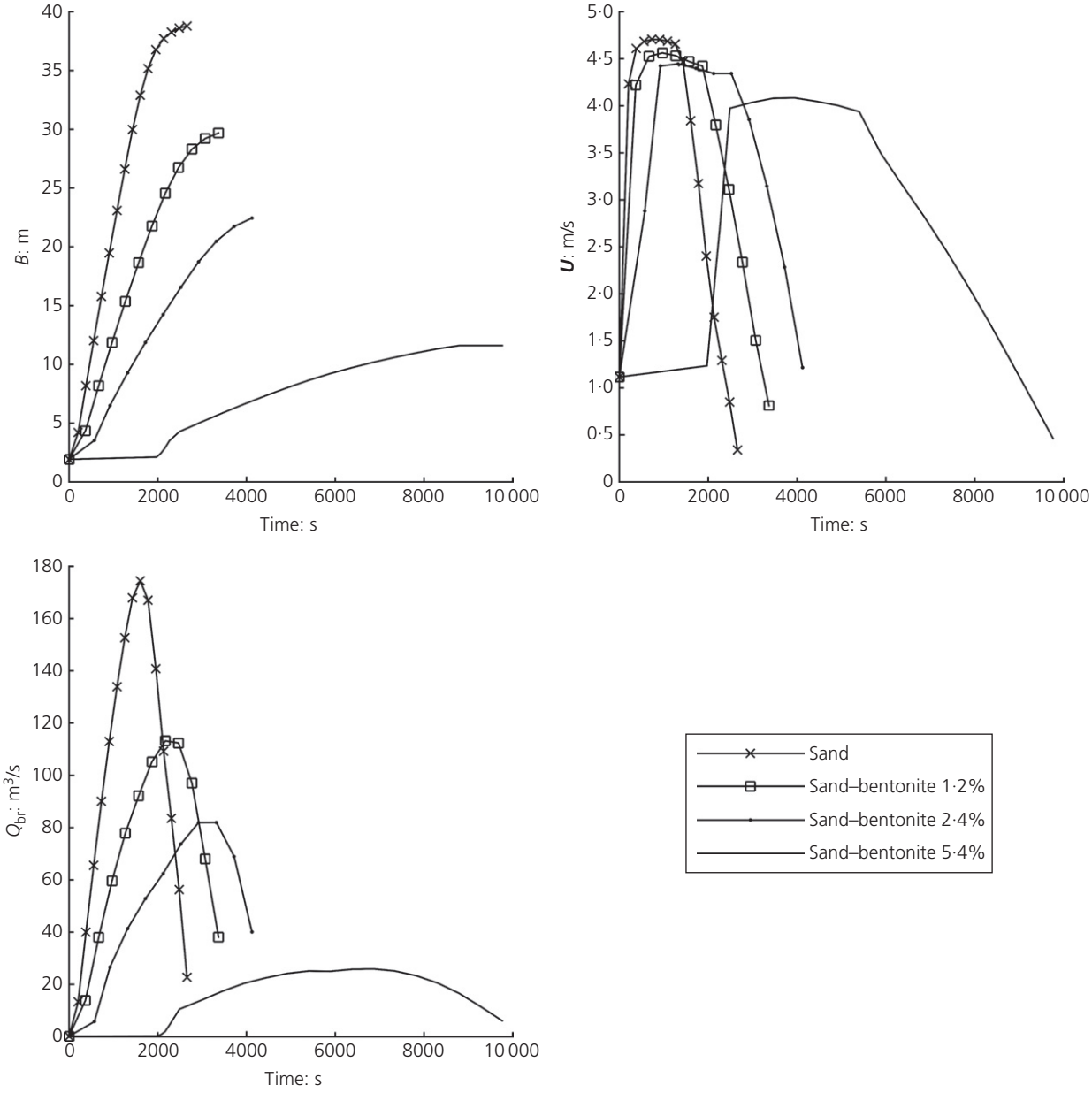

Figure 13. Comparison of Bres model results for the Zwin'94 dike for different added weight fractions of bentonite, including added bentonite percentage of 5·4%

dike, a bentonite percentage could be determined for which the breaching process does not pass stage II.

To show that the calculated bentonite percentage could reduce the inundation velocity sufficiently, a second simulation was run. This time, the outside water level was programmed to remain at a higher level for a longer period of time to ensure a fully developing breach. A comparison with the results of the other mixtures is shown in Figure 13. The inundation velocities of all mixtures are shown in Figure 14.

The results show that a sand–bentonite mixture with an added bentonite weight percentage of 5·4% reduces the inundation velocity below the threshold value of 0·5 m/h. Based on Jonkman (2004), this results in a mortality of <1%, which is a reduction by a factor of 10 compared with an unimproved sand dike.

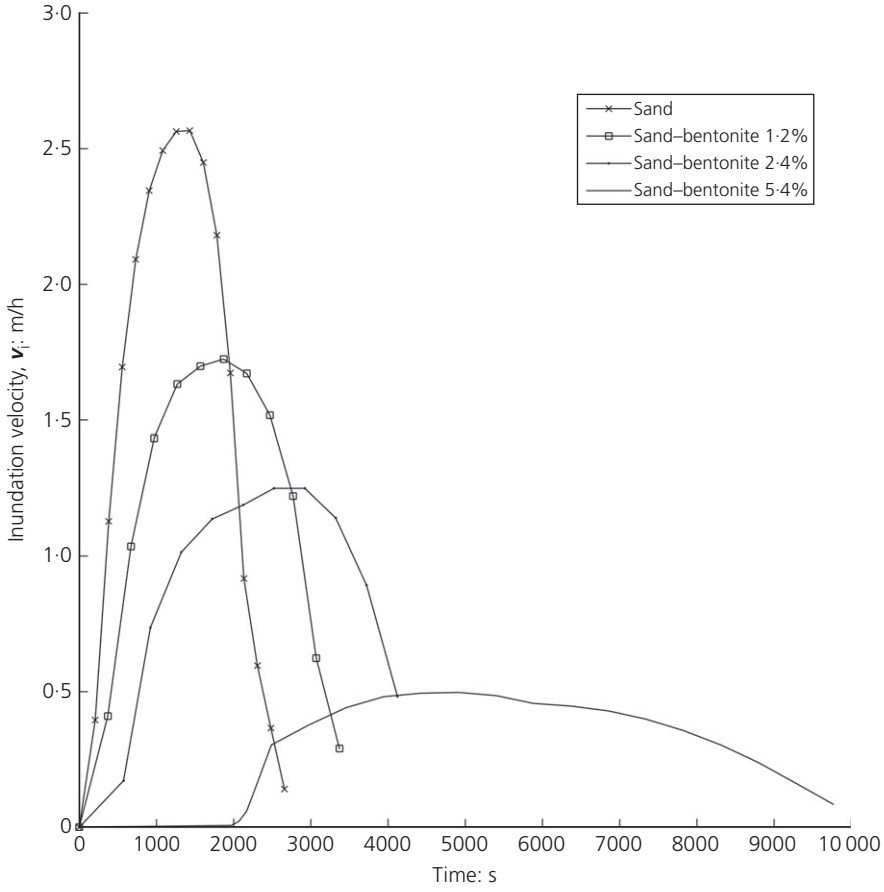

Figure 14. Comparison of inundation velocities in the Zwin'94 polder for different added weight fractions of bentonite, including necessary mixture (added bentonite percentage of 5·4%)

It should be noted that this result is only applicable for the dike, polder and circumstances of the Zwin'94 experiment.

7. Conclusions

The rate of breach development and the resulting rate of inundation in a polder will be significantly reduced when bentonite is added to the sandy core of a dike. Depending on the circumstances, this may result in a significant decrease in mortality and thus a significant increase in safety. A reduction of the erosion velocity of sand was achieved without changing the original behaviour of the sand. The direct shear tests and erosion tests indicate that the sand–bentonite mixtures still show sand-like behaviour; only the permeability is decreased by adding bentonite. This is favourable as it means that the stability of sand dikes will not change when the sand is mixed with small amounts of bentonite.

An added bentonite percentage of 2·4% will result in a significant reduction in erosion velocity. This is a promising result and could be used to slow down the breaching process of a sand dike. The model results show that just a small percentage of added bentonite achieves a significant decrease in important breach parameters and may even stop the breaching process completely. Retarding the breaching process reduces the inundation velocity in a polder. This results in decreased mortality or risk. The reduction of this risk means an increase in safety for the inhabitants of a polder. The necessary amount of bentonite to increase the safety to a desired level is different for each case. An initial estimation of the cost of improving a dike using bentonite compared with traditional dike reinforcement shows that the cost of using bentonite is approximately the same as that of traditional dike reinforcement, while the same safety level is achieved (Lemmens, 2014). Also, compared with traditional dike reinforcement, a bentonite-improved dike does not require additional space relative to the original dike profile.

This study has shown that 5·4% of bentonite results in a reduction of mortality by a factor of 10. This percentage,

however, is based on extrapolation of the present data. Erosion tests with sand and a bentonite percentage of 5·4% at higher flow velocities are necessary to confirm this behaviour. Further laboratory tests are also necessary to confirm that the strength characteristics of the sand core are not influenced by the presence of this amount of bentonite.

It may also be concluded that, besides adding bentonite, sand with an initial small percentage of clay can have a similar effect. Because of this, it is not necessary to use clean sand for dike construction, and slightly 'polluted' sand might actually be a better option, as long as the stability of the dike is not negatively affected.

REFERENCES

Bisschop F, Visser P, Van Rhee C and Verhagen H (2010) *Erosion Due to High Flow Velocities: A Description of Relevant Processes*. Delft University of Technology, Delft, the Netherlands.

Cebo Holland BV (2014) *Cebogel Sealfix*. Cebo Holland BV, IJmuiden, the Netherlands. See http://www.cebo.com/nederland/nl/bentoniet/cebogel-sealfix.html (accessed 13/04/2016).

Cheng NS and Chua LHC (2005) Comparison of sidewall correction of bed shear stress in open-channel flows. *Journal of Hydraulic Engineering* **131(7)**: 605–609.

Deltares (2011) *Analyse van Slachtofferrisico's Waterveiligheid 21e eeuw*. Deltares, Delft, the Netherlands (in Dutch).

Gailani JZ, Jin L, McNeil J and Lick W (2001) *Effects of Bentonite on Sediment Erosion Rates*. U.S. Army Engineer Research and Development Center, Vicksburg, MS, USA, DOER Technical Notes Collection.

Holtz RD and Kovacs WD (1981) *An Introduction to Geotechnical Engineering*. Prentice-Hall, Englewood Cliffs, NJ, USA.

Jonkman SN (2004) *Methode voor de Bepaling van het Aantal Slachtoffers ten Gevolge van een Grootschalige Overstroming*. Dienst Weg- en Waterbouwkunde, Delft, the Netherlands (in Dutch).

Jonkman SN (2007) *Loss of Life Estimation in Flood Risk Management*. PhD thesis, Delft University of Technology, Delft, the Netherlands.

Lemmens DDMM (2014) *Design of a Breach Retardant Dike*. MSc thesis, Department of Hydraulic Engineering, Delft University of Technology, Delft, the Netherlands.

Morris MW, Hassan MAAM, Kortenhaus A and Visser PJ (2009) *Breaching Processes: A State of the Art Review*. HR Wallingford, Wallingford, UK, FLOODsite Report T06-06-03.

Peeters P, Van Hoestenberghe T, Vincke L and Visser P (2011) SWOT analysis of breach models for common dike failure mechanisms. In *34th IAHR World Congress 2011: Balance and Uncertainty: Water in a Changing World* (Valentine E (ed.)). International Association for Hydro-Environment Engineering and Research (IAHR), Madrid, Spain, paper 3936.

Rijkswaterstaat (2006) *DWW-2006-012: Veiligheid Nederland in Kaart – Inschatting van het Aantal Slachtoffers ten Gevolge van Overstroming*. Rijkswaterstaat, Ministry of Transport, Public Works and Water Management, Utrecht, the Netherlands (in Dutch).

Van Rhee C (2010) Sediment entrainment at high flow velocity. *Journal of Hydraulic Engineering* **136(9)**: 572–582.

Van Rhee C and Talmon AM (2010) Sedimentation and erosion of sediment at high solids concentrations. In *Proceedings of the 18th International Conference on Hydrotransport* (Heywood N (ed.)). BHR Group, Cranfield, UK, pp. 211–222.

Van Rijn LC (1984) Sediment transport, part I: bed load transport. *Journal of Hydraulic Engineering, ASCE* **110(10)**: 1431–1456.

Visser PJ (1998) *Breach Growth in Sand-Dikes*. PhD thesis, Delft University of Technology, Delft, the Netherlands.

WHAT DO YOU THINK?

To discuss this paper, please email up to 500 words to the editor at journals@ice.org.uk. Your contribution will be forwarded to the author(s) for a reply and, if considered appropriate by the editorial panel, will be published as discussion in a future issue of the journal.

Proceedings journals rely entirely on contributions sent in by civil engineering professionals, academics and students. Papers should be 2000–5000 words long (briefing papers should be 1000–2000 words long), with adequate illustrations and references. You can submit your paper online via www.icevirtuallibrary.com/content/journals, where you will also find detailed author guidelines.